Therapeutics and Clinical Risk Management

Dovepress
Taylor & Francis Group

Open Access Full Text Article

ORIGINAL RESEARCH

Risk Factors for Pleural Reaction in CT-Guided Percutaneous Lung Nodule Localization: A Single-Center Retrospective Study

Ning Zhou[1,*], Nan Feng[2,*], Zichen Jiao[3], Xiaoming Shi[1], Tao Wang[1,3], Gefei Zhao[3]

[1]Department of Thoracic Surgery, Nanjing Drum Tower Clinical College of Nanjing Medical University, Nanjing, People's Republic of China; [2]Department of Radiology, Nanjing Drum Tower Hospital, Medical School, Nanjing University, Nanjing, People's Republic of China; [3]Department of Thoracic Surgery, Nanjing Drum Tower Hospital, Medical School, Nanjing University, Nanjing, People's Republic of China

*These authors contributed equally to this work

Correspondence: Gefei Zhao; Tao Wang, Department of Thoracic Surgery, Nanjing Drum Tower Hospital, No. 359 Puzhu Middle Road, Pukou District, Nanjing, Jiangsu, 210000, People's Republic of China, Email zgf6160@sina.com; wangtao_pumc@live.cn

Background: Pleural reaction (PR) frequently occurs during computed tomography (CT) -guided lung puncture procedures, and its development is influenced by various factors. This study aims to identify the risk factors associated with PR in CT-guided percutaneous lung nodule localization (CT-PLNL) procedures.

Methods: This retrospective study included 467 patients who underwent video-assisted thoracic surgery (VATS) at Nanjing Drum Tower Hospital between January 2022 and December 2023, all of whom had received CT-PLNL. Clinical data, including medical records, imaging findings, and laboratory results, were collected. Univariate analysis and Least Absolute Shrinkage and Selection Operator (LASSO) regression identified independent risk factors for PR. Binary logistic regression was performed to further analyze these factors. Receiver Operating Characteristic (ROC) curves were plotted to assess model performance, and Bootstrap validation evaluated discriminative ability. Calibration curves and decision curve analysis (DCA) were conducted to compare predicted versus actual probabilities and assess clinical applicability.

Results: The incidence of PR was 5.35% (25/467). Significant variables from univariate analysis and LASSO regression were analyzed by logistic regression. Age, intrapulmonary needle path adjustment, inadequate anesthesia, and a history of diabetes were identified as independent risk factors for PR. ROC curves showed Area Under the Curve (AUC) values indicating excellent discriminative ability. Calibration curves showed appropriate fit, and DCA demonstrated high clinical applicability.

Conclusion: Younger age groups, intraprocedural needle adjustments, inadequate anesthesia, and diabetes were independent risk factors for PR after CT-PLNL. Optimizing anesthesia, avoiding unnecessary needle manipulations, and perioperative glucose monitoring in diabetic patients may mitigate PR risks and enhance procedural safety.

Keywords: pleural reaction, lung nodule, puncture localization, risk factors, LASSO

Introduction

Lung cancer is one of the leading causes of cancer-related fatalities.[1,2] However, with the widespread use of low-dose computed tomography (LDCT), many individuals with early-stage lung cancer are now identified and treated promptly.[3,4]

Although lobectomy has long been the standard of care for lung cancer, recent research has shown that sublobar resection, including wedge resection and anatomical segmental resection, not only preserves lung function in patients with early-stage lung cancer but also improves patient survival.[5–8] Notably, precise lesion identification during surgery is crucial for the success of sublobar resection. The use of palpation to locate lesions has become increasingly inadequate, particularly with the advent of video-assisted thoracic surgery (VATS).[9] Moreover, many small pulmonary nodules located deep within the lung parenchyma are difficult to detect visually,[10] especially small, purely ground-glass nodules.

Received: 4 February 2025
Accepted: 3 July 2025
Published: 22 July 2025

To ensure accurate lesion removal during sublobar resections, preoperative CT-guided percutaneous lung nodule localization (CT-PLNL) is frequently used.[11,12] However, clinical studies have shown that many patients undergoing CT-PLNL experience adverse effects such as discomfort, coughing, and hemoptysis. In some cases, life-threatening complications such as shock, hemothorax, pneumothorax, and air embolism can occur.[13–17] One of the complications that may be easily overlooked during and after lung puncture is pleural reaction (PR), due to its subtle and atypical symptoms. More significantly, delayed diagnosis and treatment of PR can result in poor prognosis or rapid deterioration of the patient's condition.[18,19] Therefore, we believe that PR caused by CT-PLNL deserves greater attention.

To date, there have been relatively few studies on the risk factors for PR associated with CT-PLNL. One potential reason for this is that the CT-PLNL procedure is typically short and the lesions are often superficial, which results in relatively few symptoms or severe complications in patients.[20] This may partially explain why PR is more frequently reported in studies related to complications following lung tumor biopsy, ablation therapy, and radioactive particle implantation.[19,21,22] However, we note that in clinical practice, many patients require a prolonged wait for surgical intervention after CT-PLNL. During this period, delayed PR can still lead to surgical delays and even pose a threat to patient life. Therefore, this study aims to explore the risk factors for PR during the CT-PLNL process, with the goal of providing more constructive insights for clinical management.

Methods

Study Population

Clinical data from 467 patients who underwent CT-PLNL prior to lung surgery at the Department of Thoracic Surgery, Nanjing Drum Tower Hospital, Nanjing, China, between January 2022 and December 2023, were included in this retrospective cohort analysis. The study was approved by the Medical Ethics Committee of Drum Tower Hospital Affiliated to Nanjing University School of Medicine (No. 2024–379-01). Informed consent was routinely obtained from patients prior to surgery.

In this study, PR was defined as a constellation of symptoms occurring during lung-related puncture, including dizziness, sweating, pallor, palpitations, a thready pulse, cold extremities, hypotension, collapse, and, in severe cases, altered consciousness.[19,23]

Clinical Information

Using our hospital's electronic medical record system (HIS), we systematically collected and analyzed comprehensive clinical data on the included patients. These data encompassed baseline characteristics, including but not limited to gender, age, body mass index (BMI), long-term smoking and alcohol consumption, drug allergies, previous neoadjuvant therapy, history of hormone therapy, and the presence of concomitant lung-related diseases such as emphysema, asthma, chronic obstructive pulmonary disease (COPD), pulmonary bulla, interstitial pulmonary fibrosis, or abnormal pleural changes. Additionally, we recorded comorbid conditions such as cardiac arrhythmias, coronary artery disease, diabetes, hypertension, immune system disorders, and peripheral vascular disease, as well as any history of thoracic surgery.

For the localization of pulmonary nodules, we meticulously documented the imaging data, including the following specific details: the exact location of the lesion (classified as right upper, right middle, right lower, left upper, or left lower), the radiological characteristics of the nodule (ground-glass opacity, solid, or part-solid), the pulmonary classification of the lesion (left lung or right lung as Category I, and upper, middle, or lower lobe as Category II), the diameter of the lesion (based on preoperative CT reports from our hospital), the relative position of the lesion to the nearest blood vessels (particularly whether the distance to any vessel exceeds 1 cm), the patient's position during the procedure (supine, prone, left lateral, or right lateral), the actual puncture distance (the straight-line distance from the pleural entry point to the needle tip), the thickness of the chest wall (the distance from the skin entry point to the pleural entry point), whether needle adjustment was performed during the procedure, the adequacy of anesthesia, and whether any complications, such as pneumothorax or localized hematoma after needle withdrawal, occurred.

For laboratory tests, we comprehensively evaluated preoperative parameters, including fasting blood glucose (FBG) (measured on a day other than the puncture), prothrombin time (PT), D-dimer concentration, platelet count, triglyceride

levels, and liver and kidney function markers. Pulmonary function was assessed through measurements of FEV1 predicted (the expected forced expiratory volume in 1 second based on normative demographic factors) and DLCO predicted (the predicted diffusing capacity of the lungs for carbon monoxide based on normative demographic factors), to evaluate lung health. Finally, the American Society of Anesthesiologists (ASA) classification for each patient was recorded as an important reference for subsequent surgical and anesthetic management.

CT-Guided Percutaneous Localization

All CT-PLNL procedures in this study were performed by a single senior thoracic surgeon with over a decade of experience in CT-guided interventional techniques, who has independently conducted more than 1,000 lung nodule localization procedures. The CT scanner used was the IQon Spectral CT scanner, manufactured by Philips in the Netherlands. The scanning parameters were set to 1 mm layer thickness, 100 kV voltage, and 120 mA current.[24] Once the lesion location was identified by reviewing the patient's most recent preoperative diagnostic CT report, the patient was instructed to adopt the optimal position for the best exposure of the target area. The optimal puncture path was then planned using the lung window images, with assistance from an imaging specialist, to determine the exact depth of the needle and ensure the path avoided intrapulmonary vascular structures (Supplementary Figure 1).

To enhance the accuracy of the puncture, the built-in localization line of the scanner was combined with a custom-made radiopaque grid to mark the patient's body surface. Once the marking was completed, a sterile cavity towel was placed, and the marked area was disinfected three times from the inside out using iodine povidone. After local anesthesia with 2% lidocaine hydrochloride, a soft-wire hook puncture needle (20 G × 100 mm; Ningbo Shengjiekang Biotech Co., Ltd., Ningbo, China) was used for the localization procedure. The needle's length was adjusted to match the predetermined depth.

A CT scan was immediately performed after the puncture to assess the need for the direct release of the localization needle based on lung window images. If the puncture path deviated significantly—meaning the localization needle was distant from the lesion site or extended over several levels—fine-tuning was required before the needle could be released. Following successful release, the puncture tool was removed, and gauze was applied to the puncture site. A repeat CT scan was conducted to confirm the proper positioning of the localization needle in relation to the lesion and to assess the patient for potential complications such as intrapulmonary bleeding or pneumothorax.

All patients were required to stay in the CT room's rest area for 15 minutes after the procedure. During this period, experienced nursing staff closely monitored patients for abnormalities. The diagnosis of PR was strictly based on predefined multisymptom criteria (eg, hypotension, pallor, profuse sweating) and temporal correlation with the procedure. For patients with mild PR, supportive measures, such as oxygenation and careful monitoring, were generally sufficient. However, patients with severe PR required rapid intravenous rehydration, ongoing vital sign monitoring, and, if necessary, hormone therapy to stabilize their condition. Representative imaging findings of PR-associated changes in a patient undergoing CT-PLNL were shown (Supplementary Figure 2).

Statistical Analysis

This study used R (version 4.1.3) and several R packages, including comparegroups, tidyverse, glmnet, proc, rms, rmda, and ggplot2, to perform critical statistical analyses. The Shapiro–Wilk test was initially applied to assess the normality of the data. For non-normally distributed data, the Wilcoxon rank-sum test was used, and results were expressed as median with interquartile range. For normally distributed data, *t*-tests were performed, with results presented as mean ± standard deviation. Count data were expressed as percentages, and the chi-square test was employed to detect group differences.

Univariate analysis was initially conducted to identify variables that were statistically significant ($p < 0.05$) in the preliminary analysis. To refine the selection of variables, this study used the Least Absolute Shrinkage and Selection Operator (LASSO) regression model for further variable screening. Subsequently, binary logistic regression analysis was performed on the selected risk factors from both models to comprehensively examine the relationships and impacts of these variables.

A prediction model was developed based on the regression coefficients of the independent factors. The model's performance was visualized using the Receiver Operating Characteristic (ROC) curve, and the Area Under the Curve

(AUC) was calculated to objectively evaluate its discriminatory ability. Additionally, calibration curves were constructed to compare the observed and predicted probabilities. Finally, Decision Curve Analysis (DCA) was conducted to assess the model's clinical utility and its potential application in real-world decision-making. Statistical significance was defined as $p < 0.05$ in all analyses.

Results

The current study included 467 individuals who had undergone CT-PLNL, of whom 25 (5.35%) experienced PR. The vital signs of each patient at the onset of PR, the time of occurrence, and the emergency treatment measures were carefully documented (Supplementary Table 1). Univariate analysis revealed that the occurrence of PR was significantly associated with the following factors ($P < 0.05$): patient age, intrapulmonary needle adjustment, adequacy of anesthesia, preoperative fasting glucose level, history of diabetes mellitus, puncture position (prone), lesion location (upper or lower left), lesion classification II (lower lobe), and hematoma formation following needle retraction (Table 1). Further binary logistic regression analysis identified the following independent risk factors for PR ($P < 0.05$): age (OR = 0.952; 95% CI = 0.917–0.987; P = 0.009), preoperative FBG (OR = 0.424; 95% CI = 0.187–0.834; P = 0.025), history of diabetes (OR = 4.741; 95% CI = 1.316–16.322; P = 0.014), inadequate anesthesia (OR = 0.350; 95% CI = 0.130–0.926; P = 0.034),

Table 1 Clinical Characteristics of Study Population

Variables	Post-CT-PLNL Pleural Reaction		P
	NO (n=442)	YES (n=25)	
Baseline characteristics			
Gender, n (%)			0.081
Female	267 (60.4)	20 (80.0)	
Male	175 (39.6)	5 (20.0)	
Age (year)	58.0 (49.0–65.8)	49.0 (36.0–56.0)	<0.001
Age range, n (%)			0.008
≤50yrs	129 (29.2)	14 (56.0)	
>50yrs and ≤70 yrs	255 (57.7)	11 (44.0)	
>70yrs	58 (13.1)	0 (0.00)	
BMI (kg/m²)	23.4 (21.3–25.6)	23.7 (22.6–26.8)	0.272
ASA classification, n (%)			0.348
I	216 (48.9)	16 (64.0)	
II	212 (48.0)	9 (36.0)	
III	14 (3.17)	0 (0.00)	
FEV1 predicted, n (%)	87.4 (76.8–97.7)	82.6 (72.7–92.1)	0.255
FEV1 predicted range, n (%)			0.485
≤60	11 (2.49)	0 (0.00)	
>60 and ≤80	129 (29.2)	10 (40.0)	
>80	302 (68.3)	15 (60.0)	
DLCO predicted, n (%)	80.3 (69.3–92.1)	81.3 (76.8–93.4)	0.320
DLCO predicted range, n (%)			0.531
≤60	48 (10.9)	3 (12.0)	
>60 and ≤80	171 (38.7)	7 (28.0)	
>80	223 (50.5)	15 (60.0)	
Diagnosis, n (%)			1
Benign	81 (18.3)	4 (16.0)	
Malignant	361 (81.7)	21 (84.0)	
Emphysema, n (%)			0.063
Yes	84 (19.0)	1 (4.00)	
No	358 (81.0)	24 (96.0)	

(*Continued*)

Table 1 (Continued).

Variables	Post-CT-PLNL Pleural Reaction		P
	NO (n=442)	YES (n=25)	
Asthma, n (%)			1
Yes	6 (1.36)	0 (0.00)	
No	436 (98.6)	25 (100)	
COPD, n (%)			0.568
Yes	14 (3.17)	1 (4.00)	
No	428 (96.8)	24 (96.0)	
Pulmonary bulla, n (%)			1
Yes	22 (4.98)	1 (4.00)	
No	420 (95.0)	24 (96.0)	
Interstitial pulmonary fibrosis, n (%)			1
Yes	1 (0.23)	0 (0.00)	
No	441 (99.8)	25 (100)	
Abnormal pleural changes, n (%)			0.085
Yes	112 (25.3)	2 (8.00)	
No	330 (74.7)	23 (92.0)	
Cardiac arrhythmias, n (%)			0.594
Yes	80 (18.1)	3 (12.0)	
No	362 (81.9)	22 (88.0)	
Coronary artery disease, n (%)			0.386
Yes	27 (6.11)	0 (0.00)	
No	415 (93.9)	25 (100)	
Hypertension, n (%)			0.754
Yes	110 (24.9)	5 (20.0)	
No	332 (75.1)	20 (80.0)	
Peripheral vascular disease, n (%)			1
Yes	23 (5.20)	1 (4.00)	
No	419 (94.8)	24 (96.0)	
Immune system disorders, n (%)			0.426
Yes	9 (2.04)	1 (4.00)	
No	433 (98.0)	24 (96.0)	
Diabetes, n (%)			0.019
Yes	48 (10.9)	7 (28.0)	
No	394 (89.1)	18 (72.0)	
Abnormal liver function, n (%)			0.261
Yes	37 (8.37)	4 (16.0)	
No	405 (91.6)	21 (84.0)	
Renal insufficiency, n (%)			0.229
Yes	63 (14.3)	1 (4.00)	
No	379 (85.7)	24 (96.0)	
Hyperlipidemia, n (%)			1
Yes	192 (43.4)	11 (44.0)	
No	250 (56.6)	14 (56.0)	
Drug allergies, n (%)			0.366
Yes	59 (13.3)	5 (20.0)	
No	383 (86.7)	20 (80.0)	
History of thoracic surgery, n (%)			1
Yes	47 (10.6)	2 (8.00)	
No	395 (89.4)	23 (92.0)	

(*Continued*)

https://doi.org/10.2147/TCRM.S516329

Table 1 (Continued).

Variables	Post-CT-PLNL Pleural Reaction		P
	NO (n=442)	YES (n=25)	
Long-term smoking, n (%)			1
Yes	52 (11.8)	3 (12.0)	
No	390 (88.2)	22 (88.0)	
Long-term alcohol consumption, n (%)			1
Yes	34 (7.69)	1 (4.00)	
No	408 (92.3)	24 (96.0)	
Neoadjuvant therapy, n (%)			0.282
Yes	5 (1.13)	1 (4.00)	
No	437 (98.9)	24 (96.0)	
History of hormone therapy, n (%)			1
Yes	2 (0.45)	0 (0.00)	
No	440 (99.5)	25 (100)	
Blood test			
PT (s)	11.1 (10.8–11.6)	11.3 (10.9–11.9)	0.139
D-Dimer (mg/mL)	0.45 (0.24–0.72)	0.63 (0.41–0.81)	0.129
PLT (x10^9/L)	197 (161–234)	196 (170–240)	0.975
Blood glucose (mmol/L)	4.88 (4.51–5.45)	4.41 (4.17–4.96)	0.002
Blood glucose range, n (%)			0.003
≤4.58mmol/L	138 (31.2)	16 (64.0)	
>4.58 and ≤5.20mmol/L	151 (34.2)	5 (20.0)	
>5.20mmol/L	153 (34.6)	4 (16.0)	
Imaging examination			
Lesion diameter (mm)	9.70 (8.45–11.9)	9.30 (8.21–9.87)	0.099
Puncture distance (mm)	13.1 (9.61–17.1)	14.1 (7.23–20.6)	0.913
Chest wall thickness (mm)	37.0 (31.2–46.1)	36.9 (30.1–47.0)	0.613
Nodule characteristics, n (%)			0.535
p-GGN	287 (64.9)	17 (68.0)	
SN	121 (27.4)	5 (20.0)	
p-SN	34 (7.69)	3 (12.0)	
Exact location of the lesion, n (%)			0.014
Right upper lung	131 (29.6)	7 (28.0)	
Right middle lung	22 (4.98)	2 (8.00)	
Right lower lung	81 (18.3)	5 (20.0)	
Left upper lung	123 (27.8)	1 (4.00)	
Left low lung	85 (19.2)	10 (40.0)	
Lesion location.I, n (%)			0.817
Right lung	232 (52.5)	12 (48.0)	
Left lung	210 (47.5)	13 (52.0)	
Lesion Location.II, n (%)			0.032
Upper lung	253 (57.2)	8 (32.0)	
Middle lung	24 (5.43)	2 (8.00)	
Lower lung	165 (37.3)	15 (60.0)	
Patient positioning, n (%)			0.143
Supine	88 (19.9)	3 (12.0)	
Prone	171 (38.7)	16 (64.0)	
Left decubitus	91 (20.6)	3 (12.0)	
Right decubitus	92 (20.8)	3 (12.0)	

(*Continued*)

Table 1 (Continued).

Variables	Post-CT-PLNL Pleural Reaction		P
	NO (n=442)	YES (n=25)	
Distance from the nearest vascular, n (%)			0.596
≤1cm	84 (19.0)	3 (12.0)	
>1cm	358 (81.0)	22 (88.0)	
Intrapulmonary needle adjustment, n (%)			<0.001
Yes	57 (12.9)	11 (44.0)	
No	385 (87.1)	14 (56.0)	
Adequate anesthesia, n (%)			0.005
Yes	319 (72.2)	11 (44.0)	
No	123 (27.8)	14 (56.0)	
Post-needle withdrawal hematoma, n (%)			0.039
Yes	149 (33.7)	14 (56.0)	
No	293 (66.3)	11 (44.0)	
Post-aspiration pneumothorax, n (%)			0.390
Yes	182 (41.2)	13 (52.0)	
No	260 (58.8)	12 (48.0)	

Note: Statistically significant at P < 0.05.
Abbreviations: BMI, Body Mass Index; ASA, American Society of Anesthesiologists Physical Status; FEV1, forced expiratory volume in one second; DLCO, diffusion capacity for carbon monoxide of the lung; COPD, chronic obstructive pulmonary disease; PT, prothrombin time; PLT, platelet; p-GGN, pure ground-glass nodule; SN, solid nodule; p-SN, part-solid nodule.

intrapulmonary needle tract adjustments (OR = 5.348; 95% CI = 1.910–15.025; P = 0.001), hematoma formation following needle retraction (OR = 2.766; 95% CI = 1.056–7.416; P = 0.038), and lesion location in the lower lobe of the left lung (OR = 4.914; 95% CI = 1.309–21.775; P = 0.025) (Table 2).

The LASSO regression model with three-fold cross-validation was used to identify four risk factors with non-zero coefficients: age, anesthetic adequacy, intrapulmonary needle adjustment, and history of diabetes mellitus (Figure 1). A second binary logistic regression analysis, using the CT-PLNL concurrent PR as the dependent variable and the

Table 2 Multivariate Analysis Results (Based on Univariate Analysis)

Variables	Odds Ratio	95% CI	P
Age	0.952	0.917–0.987	0.009
Blood glucose	0.424	0.187–0.834	0.025
Diabetes	4.741	1.316–16.322	0.014
Adequate anesthesia	0.350	0.130–0.926	0.034
Intrapulmonary needle adjustment	5.348	1.910–15.025	0.001
Post-needle withdrawal hematoma	2.766	1.056–7.416	0.038
Location of nodule			
Left upper lung vs Right upper lung	0.149	0.008–0.900	0.083
Left lower lung vs Right upper lung	4.914	1.309–21.775	0.025
Lesion location.II			
Lower lobe vs Upper lobe	0.326	0.067–1.337	0.138
Patient positioning			
Prone vs Supine	1.633	0.563–4.814	0.365

Note: Statistically significant at P < 0.05.
Abbreviation: CI, confidence interval.

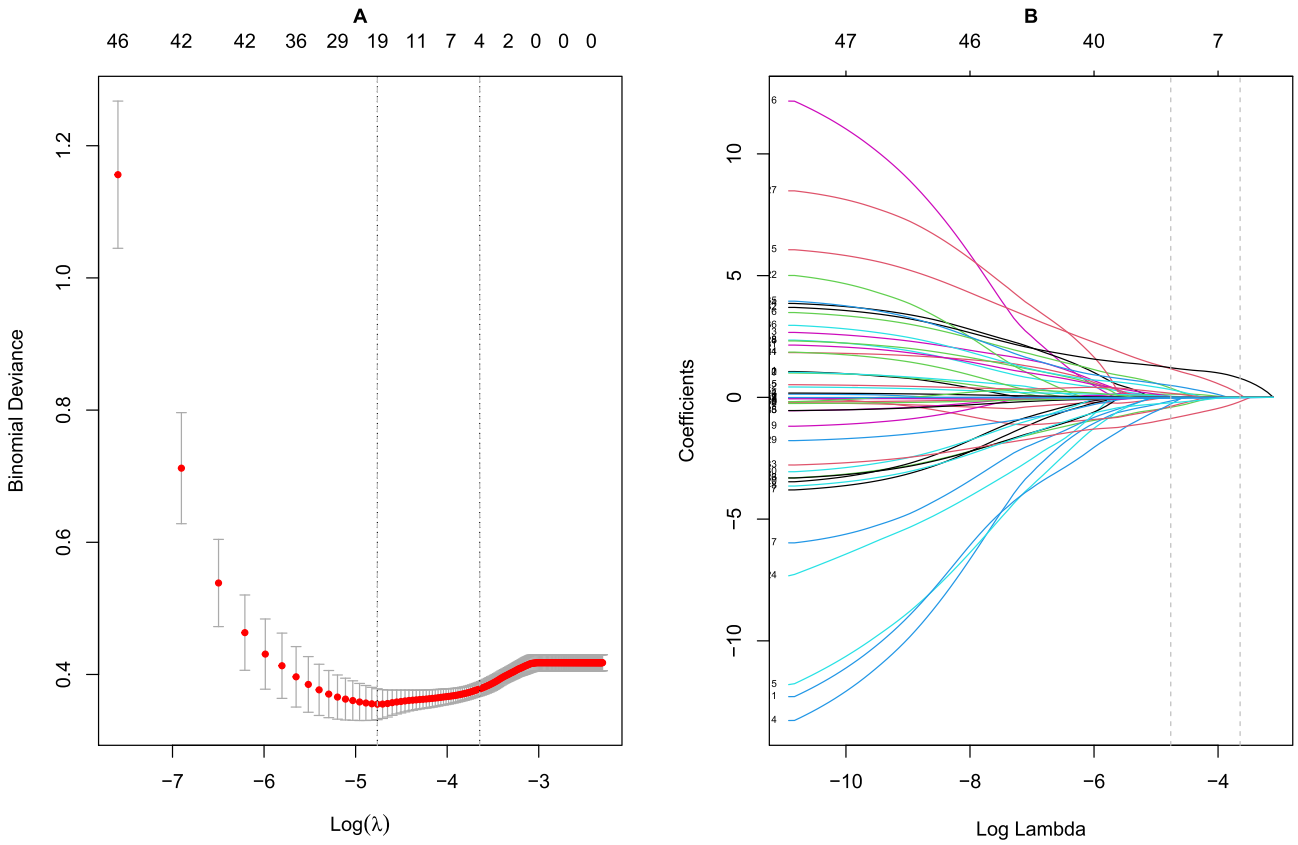

Figure 1 (**A**) Cross-validation curve of the LASSO regression model. This figure displays the cross-validation error (mean squared error) across different values of λ. The value of λ corresponding to the minimum error represents the optimal regularization strength, helping to balance model complexity and fit. (**B**) Coefficient path plot of the LASSO regression model. This plot shows how the coefficients of the model's variables change with varying regularization strength (λ). As λ increases, the coefficients of some variables gradually shrink and eventually reach zero, indicating that the LASSO regression model performs variable selection through the penalty term.The reference lines represent the smallest regularization parameter (λmin) and the value of λ that causes the error to increase by no more than one standard error (λ1-SE). Based on the 1-SE rule, this study selected four variables with non-zero coefficients as potential risk factors.
Abbreviations: LASSO, Least absolute shrinkage and selection operator; λ, Lambda; λmin, Minimum Lambda; SE, Standard Error.

aforementioned potential risk factors as independent variables, confirmed that the following factors were statistically significant (P < 0.05): age (OR = 0.941; 95% CI = 0.909–0.972; P < 0.001), history of diabetes (OR = 4.435; 95% CI = 1.457–12.685; P = 0.006), inadequate anesthesia (OR = 0.315; 95% CI = 0.128–0.762; P = 0.010), and intrapulmonary needle adjustment (OR = 5.198; 95% CI = 2.069–12.898; P < 0.001) (Table 3).

ROC curves for both models were independently generated using R software, based on the findings from the binary logistic regression analysis. The AUCs for the two models were 0.882 (95% CI: 0.811–0.952) and 0.813 (95% CI: 0.717–0.910), respectively (Figure 2). Internal validation using the bootstrap method produced AUCs of 0.881 (95% CI: 0.809–0.884) and 0.815 (95% CI: 0.717–0.817) for the two models (Supplementary Figures 3 and 4). Calibration curves

Table 3 Multivariate Analysis Results (From the LASSO Regression Analysis)

Variables	Odds Ratio	95% CI	P
Age	0.941	0.909–0.972	<0.001
Diabetes	4.435	1.457–12.685	0.006
Adequate anesthesia	0.315	0.128–0.762	0.010
Intrapulmonary needle adjustment	5.198	2.069–12.898	<0.001

Note: Statistically significant at P < 0.05.
Abbreviation: CI, confidence interval.

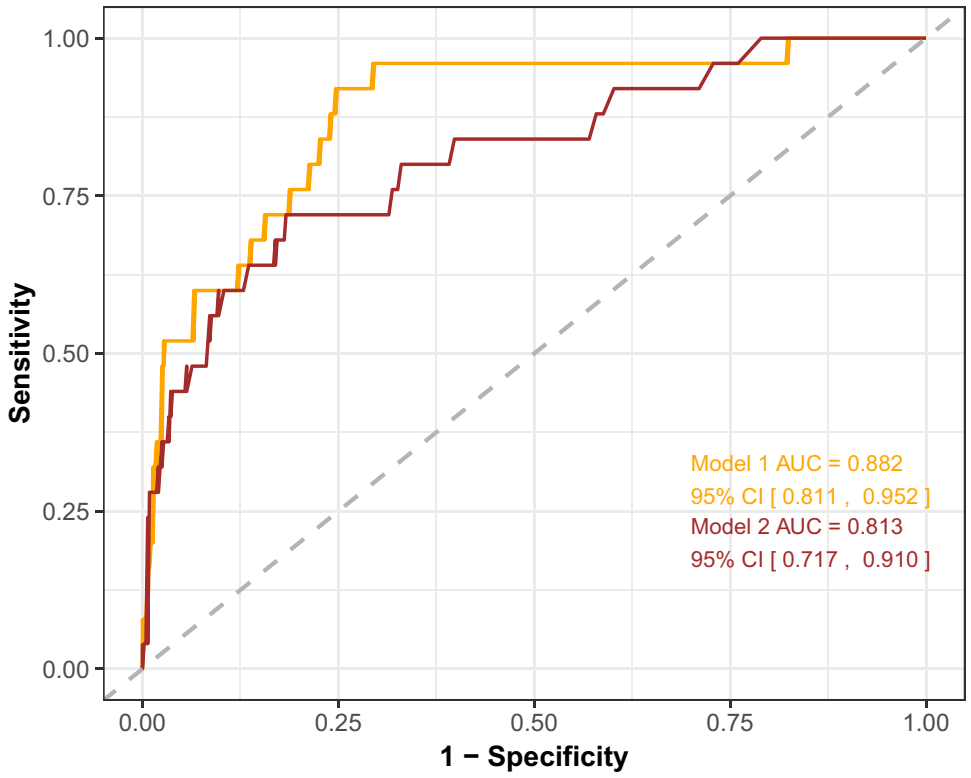

Figure 2 Receiver operating characteristic (ROC) curves for two logistic regression models. Model 1 (Orange curve) selects variables using univariate analysis, while Model 2 (brown curve) incorporates variables chosen through LASSO regression. The x-axis represents the false positive rate (1-specificity), and the y-axis denotes the true positive rate (sensitivity). Both models exhibit strong classification performance, with Model 1 slightly outperforming Model 2 across various thresholds. The diagonal line indicates the performance of random guessing, serving as a baseline for comparison.
Abbreviations: AUC, area under the curve; CI, confidence interval; ROC, Receiver Operating Characteristic; LASSO, Least absolute shrinkage and selection operator.

for the two models were plotted and subjected to the Hosmer-Lemeshow test, with a result of $P > 0.05$, indicating appropriate fit of the calibration curves for both models (Figure 3). Furthermore, the DCA suggested that both models have clinical applicability (Figure 4).

Discussion

According to previous studies, the incidence of PR during thoracentesis ranges from 5% to 46%.[25–28] While mild cases of PR may cause discomfort, more severe cases can lead to shock and, in some situations, even death.[29] Therefore, to reduce the incidence of PR and improve patient outcomes, it is critical to actively identify potential risk factors and implement targeted interventions.

The underlying mechanisms of lung puncture-related PR remain poorly understood. Some studies suggest that factors such as the patient's physical condition, pain threshold, and the operator's experience may influence the likelihood of PR.[25] This investigation employed several techniques to identify potential risk factors for PR in clinical practice and developed corresponding risk assessment models. Overall, the models demonstrated good predictive accuracy for PR incidence with satisfactory calibration. Importantly, the factors identified in both models were highly consistent from a clinical perspective.

Our findings are consistent with previous research, which suggests that younger individuals are at a higher risk of developing PR following CT-guided puncture localization of lung nodules. Additionally, the risk of PR increases when the puncture is performed in the prone position or when the lesions are located in the lower lungs.[19] While we are unable to fully explain the underlying mechanism, we speculate that more active vagal reflexes in these patients during CT-PLNL may contribute to the phenomenon, based on prior studies. However, it is important to acknowledge that some of

https://doi.org/10.2147/TCRM.S516329

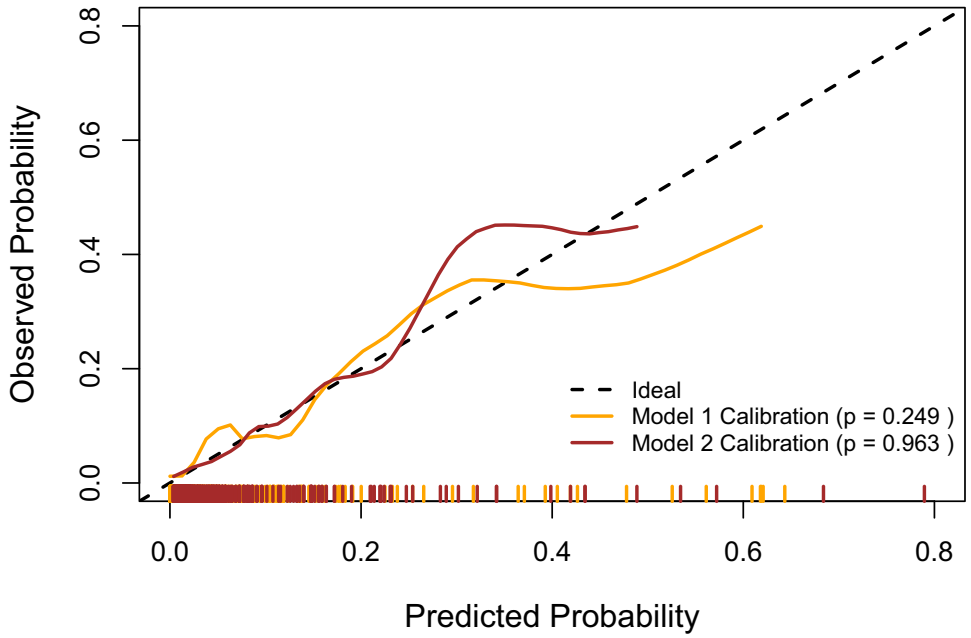

Figure 3 Calibration curves for two logistic regression models. Model 1 (Orange curve) includes variables selected via univariate analysis, while Model 2 (brown curve) utilizes variables selected through LASSO regression. Both models were calibrated using cross-validation (bootstrap method). The black dashed line represents the ideal calibration, where the predicted probabilities align perfectly with the observed outcomes. Both models show appropriate calibration, as indicated by p-values greater than 0.05 from the Hosmer-Lemeshow test. Tick marks on the x-axis (orange and brown) correspond to the predicted probabilities for Model 1 and Model 2, respectively, across the dataset.

Abbreviation: LASSO, Least absolute shrinkage and selection operator.

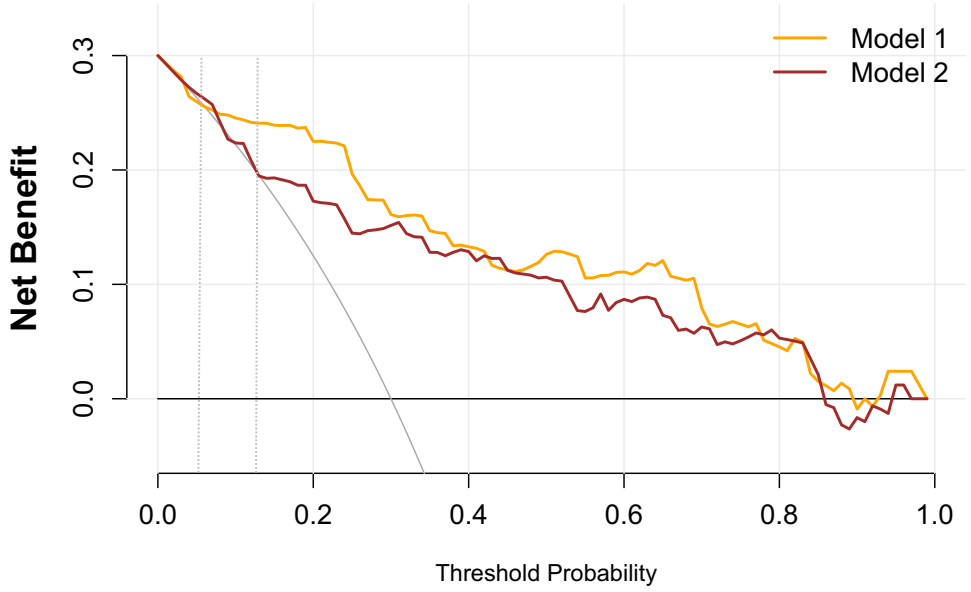

Figure 4 Decision Curve Analysis (DCA) for two logistic regression models. Model 1 (Orange line) selects variables based on univariate analysis, while Model 2 (brown line) includes variables selected through LASSO regression. The x-axis represents the threshold probability, while the y-axis shows the net benefit. Both models provide positive net benefits across a range of threshold probabilities, with Model 1 offering a higher net benefit at lower threshold values compared to Model 2. The reference line indicates the net benefit of treating all or no patients, highlighting the added value of the models in clinical decision-making.

Abbreviations: DCA, Decision Curve Analysis; LASSO, Least absolute shrinkage and selection operator.

these risk factors may be unavoidable during the procedure. Therefore, it is essential to carefully monitor the patient's complaints, symptoms, and vital signs throughout the puncture procedure, and adjust treatment as needed.

Some other risk factors identified in this study could have clinical significance in reducing PR during CT-PLNL. First, we found that adequate pleural anesthesia prior to the procedure is critical in minimizing the risk of PR. We observed that pleural anesthesia was insufficient in a significant proportion of patients (44%), as indicated by CT imaging data (Table 1). This may be due to a long skin-to-pleura distance, making it difficult for the needle tip to reach the pleura, or a lack of visible signs of drug infiltration on the pleural surface prior to puncture. To address this, we suggest using a longer syringe and continually verifying that the syringe needle has reached the pleural surface, especially when the skin-to-pleura distance is large.

Additionally, our investigation found that repeated adjustments to the puncture depth and needle direction within the lungs may be an independent risk factor for PR. This finding aligns with research on procedures such as particle implantation, biopsy, and lung tumor ablation, where repeated adjustments to the needle tract are necessary to diagnose and treat the target lesion.[19,21,22] However, in CT-PLNL, the needle tract adjustment may not be required because the resection area is typically larger than the area marked by the puncture needle, ensuring precise resection of both the lesion and the localization needle. To reduce the risk of PR, we suggest minimizing or even halting needle tract adjustments during CT-PLNL when the lesion is being radically resected at the initial puncture site.

The regression analysis results also revealed that diabetes mellitus is an independent risk factor for PR. Several patients with PR had significantly lower blood glucose levels during the course of the disease, as observed in the baseline data. Since the symptoms of PR and hypoglycemia can be quite similar, we suspect that some patients diagnosed with PR may have actually experienced hypoglycemic. Because the study dataset did not include pre-CT-PLNL blood glucose measurements for all patients, we used the first post-admission blood glucose levels to infer the pre-procedure glucose levels. Typically, patients at our center are instructed to fast after 10 p.m. the night before the procedure, which limits pre-procedure data. Nevertheless, binary logistic regression analysis revealed that low blood glucose levels were an independent risk factor for PR. Unfortunately, providing a definitive explanation for this outcome is challenging with the available data. Accurately differentiating true PR cases from hypoglycemic individuals remains diagnostically challenging due to overlapping symptom presentations. In routine clinical practice, immediate capillary blood glucose measurement is therefore mandated as a standard procedural step. Glucose supplementation therapy is initiated when values decline markedly below the established normal physiological range (<3.9 mmol/L [70 mg/dL]), with treatment efficacy monitored via continuous biochemical analyses and clinical status evaluations. It is crucial to monitor the blood glucose levels of diabetic patients and provide appropriate management prior to CT-PLNL. This subgroup of patients warrants further clinical research to better understand the relationship between blood glucose and PR.

Finally, we observed that some patients developed PR symptoms gradually after returning to the ward, such as Patient 19 in Supplementary Table 1. This delayed onset of PR is often more easily overlooked. Upon reviewing the patient's medical records, we found that this patient developed a localized pulmonary hematoma after CT-PLNL. We hypothesize that this delayed PR may be associated with postoperative pulmonary hematoma, suggesting that the presence of a pulmonary hematoma detected on an immediate postoperative chest CT following CT-PLNL could serve as an important reference for early intervention in cases of delayed PR. The risk of pulmonary vascular bleeding post-puncture cannot be entirely eliminated; however, strategic avoidance of vascular-dense regions during procedural planning is critical for complication mitigation. Enhanced monitoring of vital signs and expedited preoperative timelines are recommended upon detection of pulmonary hematoma to optimize diagnostic and management approaches for delayed PR.

There are several limitations to our study. First, as a retrospective study with limited data, we only used FBG as a proxy for pre-CT-PLNL blood glucose, which could introduce some bias. A prospective study with more rigorous data collection is needed to address this limitation. Additionally, since this study was conducted at a single institution, external validation is required to confirm the generalizability of our findings. All procedures in this investigation were performed by a single senior physician. While this methodology maximized procedural consistency, subsequent research should systematically evaluate the influence of operator experience heterogeneity on PR incidence to substantiate the broader applicability of these findings. Second, although temporal correlations were observed, the pathophysiological

mechanisms linking post-puncture pulmonary hematoma to delayed PR remain undefined, necessitating expanded mechanistic studies to clarify causal relationships. Third, although air embolism is widely acknowledged as a severe complication in lung biopsy cohorts,[30,31] large-scale systematic investigations addressing localization procedure-associated air embolism remain markedly lacking, with current knowledge predominantly relying on isolated case reports,[32] impeding precise risk stratification and evidence-based prevention strategies.

Conclusion

In summary, this study demonstrated that PR complicating CT-PLNL was associated with age, intrapulmonary needle tract adjustment, inadequate anesthesia, a history of diabetes mellitus, and the location of the lesion in the lower lobe of the left lung. Furthermore, the potential for delayed PR should be closely monitored, particularly when CT scans show the development of an intrapulmonary hematoma following needle extraction.

Data Sharing Statement

The data used and/or analyzed during the current study are available from the corresponding author on reasonable request.

Ethics Approval and Informed Consent

The study was approved by the Medical Ethics Committee of Drum Tower Hospital Affiliated to Nanjing University School of Medicine (No. 2024-379-01). Informed consent was routinely obtained from patients prior to surgery. All procedures followed the ethical standards of the Declaration of Helsinki.

Acknowledgments

We sincerely thank all patients and researchers who contributed to the study on risk factors for PR following CT-PLNL.

Author Contributions

All authors made substantial contributions to conception and design, acquisition of data, or analysis and interpretation of data; took part in drafting the article or revising it critically for important intellectual content; agreed to submit to the current journal; gave final approval of the version to be published; and agreed to be accountable for all aspects of the work.

Funding

This work was supported by fundings for clinical trials from the Affiliated Drum Tower Hospital, Medical School of Nanjing University (Grant No. 2023-LCYJ-MS-08) and the Nanjing Medical Key Science and Technology Development Project (Grant No. ZKX23015).

Disclosure

The authors declare that they have no competing interests or financial disclosures related to this study.

References

1. Kim J, Lee H, Huang BW. Lung cancer: diagnosis, treatment principles, and screening. *Am Family Phys*. 2022;105(5):487–494.
2. Bray F, Laversanne M, Sung H, et al. Global cancer statistics 2022: GLOBOCAN estimates of incidence and mortality worldwide for 36 cancers in 185 countries. *Ca a Cancer J Clinicians*. 2024;74(3):229–263. doi:10.3322/caac.21834
3. Lee E, Kazerooni EA. Lung Cancer Screening. *Semin Resp Crit Care Med*. 2022;43(6):839–850. doi:10.1055/s-0042-1757885
4. Moyer VA. Screening for lung cancer: U.S. preventive services task force recommendation statement. *Ann Internal Med*. 2014;160(5):330–338. doi:10.7326/M13-2771
5. Altorki N, Wang X, Kozono D, et al. Lobar or sublobar resection for peripheral stage IA non-small-cell lung cancer. *New Engl J Med*. 2023;388(6):489–498. doi:10.1056/NEJMoa2212083
6. Saji H, Okada M, Tsuboi M, et al. Segmentectomy versus lobectomy in small-sized peripheral non-small-cell lung cancer (JCOG0802/WJOG4607L): a multicentre, open-label, Phase 3, randomised, controlled, non-inferiority trial. *Lancet*. 2022;399(10335):1607–1617. doi:10.1016/S0140-6736(21)02333-3
7. Aokage K, Suzuki K, Saji H, et al. Segmentectomy for ground-glass-dominant lung cancer with a tumour diameter of 3 cm or less including ground-glass opacity (JCOG1211): a multicentre, single-arm, confirmatory, phase 3 trial. *Lancet Respir Med*. 2023;11(6):540–549. doi:10.1016/S2213-2600(23)00041-3

8. Suzuki K, Watanabe SI, Wakabayashi M, et al. A single-arm study of sublobar resection for ground-glass opacity dominant peripheral lung cancer. *J Thoracic Cardiovasc Surg*. 2022;163(1):289–301.e282. doi:10.1016/j.jtcvs.2020.09.146
9. Nardini M, Dunning J. Pulmonary nodules precision localization techniques. *Future Oncol*. 2020;16(16s):15–19. doi:10.2217/fon-2019-0069
10. Yang YL, Li ZZ, Huang WC, et al. Electromagnetic navigation bronchoscopic localization versus percutaneous CT-guided localization for thoracoscopic resection of small pulmonary nodules. *Thoracic Cancer*. 2021;12(4):468–474. doi:10.1111/1759-7714.13775
11. Teng F, Wang ZS, Wu AL, Fu YF, Yang S. Computed tomography-guided coil localization for video-assisted thoracoscopic surgery of sub-solid lung nodules: a retrospective study. *ANZ J Surg*. 2019;89(11):E514–e518. doi:10.1111/ans.15450
12. Manouvelou S, Mosa E, Tolia M, et al. Percutaneous computed tomography-guided localization of pulmonary nodules with hook wire prior to video-assisted thoracoscopic surgery. *J BUON*. 2019;24(1):267–272.
13. Wu CC, Maher MM, Shepard JA. Complications of CT-guided percutaneous needle biopsy of the chest: prevention and management. *AJR*. 2011;196(6):W678–682. doi:10.2214/AJR.10.4659
14. Khan MF, Straub R, Moghaddam SR, et al. Variables affecting the risk of pneumothorax and intrapulmonal hemorrhage in CT-guided transthoracic biopsy. *Eur Radiol*. 2008;18(7):1356–1363. doi:10.1007/s00330-008-0893-1
15. Yeow KM, Su IH, Pan KT, et al. Risk factors of pneumothorax and bleeding: multivariate analysis of 660 CT-guided coaxial cutting needle lung biopsies. *Chest*. 2004;126(3):748–754. doi:10.1378/chest.126.3.748
16. Sinner WN. Complications of percutaneous transthoracic needle aspiration biopsy. *Acta Radiolog Diagnos*. 1976;17(6):813–828. doi:10.1177/028418517601700609
17. Perlmutt LM, Johnston WW, Dunnick NR. Percutaneous transthoracic needle aspiration: a review. *AJR*. 1989;152(3):451–455. doi:10.2214/ajr.152.3.451
18. Heerink WJ, de Bock GH, de Jonge GJ, Groen HJ, Vliegenthart R, Oudkerk M. Complication rates of CT-guided transthoracic lung biopsy: meta-analysis. *Eur Radiol*. 2017;27(1):138–148. doi:10.1007/s00330-016-4357-8
19. Wang S, Tu J, Dong K. Nomogram to predict postoperative PR in patients undergoing CT-guided transthoracic lung biopsy. *J Thoracic Dis*. 2019;11(4):1705–1713. doi:10.21037/jtd.2019.01.60
20. Huang JY, Tsai SC, Wu TC, Lin FC. Puncture frequency predicts pneumothorax in preoperative computed tomography-guided lung nodule localization for video-assisted thoracoscopic surgery. *Thoracic Cancer*. 2022;13(13):1925–1932. doi:10.1111/1759-7714.14457
21. Yang DY, Lin YP, Xue C, et al. CT-guided percutaneous implantation of (125)I particles in treatment of early lung cancer. *J Thoracic Dis*. 2020;12(10):5996–6009. doi:10.21037/jtd-20-2666
22. Wang Y, Li W, He X, Li G, Xu L. Computed tomography-guided core needle biopsy of lung lesions: diagnostic yield and correlation between factors and complications. *Oncol Lett*. 2014;7(1):288–294. doi:10.3892/ol.2013.1680
23. Wang Y, Zhang Y, Ren N, et al. Repeat biopsy versus initial biopsy in terms of complication risk factors and clinical outcomes for patients with non-small cell lung cancer: a comparative study of 113 CT-guided needle biopsy of lung lesions. *Front Oncol*. 2024;14:1367603. doi:10.3389/fonc.2024.1367603
24. Feng Q, Zhou J, Dong N, et al. Factors influencing the accuracy and safety of preoperative computed tomography (CT)-guided soft hook-wire localization for pulmonary nodules: a comprehensive analysis. *Quant Imaging Med Surg*. 2024;14(3):2309–2320. doi:10.21037/qims-23-1272
25. Collins TR, Sahn SA. Thoracocentesis clinical value, complications, technical problems, and patient experience. *Chest*. 1987;91(6):817–822. doi:10.1378/chest.91.6.817
26. Cao W, Wang Y, Zhou N, Xu B. Efficacy of ultrasound-guided thoracentesis catheter drainage for pleural effusion. *Oncol Lett*. 2016;12(6):4445–4448. doi:10.3892/ol.2016.5244
27. Chakrabarti B, Earis JE, Pandey R, et al. Risk assessment of pneumothorax and pulmonary haemorrhage complicating percutaneous co-axial cutting needle lung biopsy. *Respir Med*. 2009;103(3):449–455. doi:10.1016/j.rmed.2008.09.010
28. Yamagami T, Nakamura T, Iida S, Kato T, Nishimura T. Management of pneumothorax after percutaneous CT-guided lung biopsy. *Chest*. 2002;121(4):1159–1164. doi:10.1378/chest.121.4.1159
29. Cantey EP, Walter JM, Corbridge T, Barsuk JH. Complications of thoracentesis: incidence, risk factors, and strategies for prevention. *Curr Opin Pulm Med*. 2016;22(4):378–385. doi:10.1097/MCP.0000000000000285
30. Lee JH, Yoon SH, Hong H, Rho JY, Goo JM. Incidence, risk factors, and prognostic indicators of symptomatic air embolism after percutaneous transthoracic lung biopsy: a systematic review and pooled analysis. *Eur Radiol*. 2021;31(4):2022–2033. doi:10.1007/s00330-020-07372-w
31. Ahn Y, Lee SM, Kim HJ, et al. Air embolism in CT-guided transthoracic needle biopsy: emphasis on pulmonary vein injury. *Eur Radiol*. 2022;32(10):6800–6811. doi:10.1007/s00330-022-09079-6
32. Wang MY, Liu YS, An XB, Li K, Liu YJ, Wang F. Cerebral arterial air embolism after computed tomography-guided hook-wire localization of a pulmonary nodule: a case report. *Medicine*. 2019;98(18):e15437. doi:10.1097/MD.0000000000015437